Volume 12
Number 13
7 July 2022
Pages 4089–4402

Catalysis Science & Technology

rsc.li/catalysis

ISSN 2044-4761

ROYAL SOCIETY OF CHEMISTRY

PAPER
Valérie Toussaint and Irina Delidovich
Revealing the contributions of homogeneous and heterogeneous catalysis to isomerization of D-glucose into D-fructose in the presence of basic salts with low solubility

Catalysis Science & Technology

ROYAL SOCIETY OF CHEMISTRY

PAPER

View Article Online
View Journal | View Issue

Open Access Article. Published on 04 May 2022. Downloaded on 10/16/2025 5:20:47 PM.
This article is licensed under a Creative Commons Attribution-NonCommercial 3.0 Unported Licence.

Check for updates

Cite this: *Catal. Sci. Technol.*, 2022, **12**, 4118

Revealing the contributions of homogeneous and heterogeneous catalysis to isomerization of D-glucose into D-fructose in the presence of basic salts with low solubility†

Valérie Toussaint [ab] and Irina Delidovich *[ab]

Received 22nd March 2022,
Accepted 4th May 2022

DOI: 10.1039/d2cy00551d

rsc.li/catalysis

Isomerization of D-glucose (Glc) into D-fructose (Fru) presents an important step in the catalytic valorization of cellulosic biomass. However, a rational catalyst design for isomerization poses a challenge. In this work, we studied the catalytic activity of basic salts with low solubility Li_2CO_3, $MgCO_3$, Li_3PO_4, $SrCO_3$, $CaCO_3$, $BaCO_3$, and $Mg_3(PO_4)_2$ for Glc isomerization into Fru. In bulk water, these materials generate OH^- *via* partial dissolution and protonation of the anions. The catalysts were tested for isomerization using 10 wt% aqueous Glc solution at 60 and 80 °C. The initial rate of Fru formation $r_{0,Fru}$ shows an excellent correlation with the initial pH values of the reaction mixtures, indicating *in situ* generated OH^- anions as catalytically active species. Filtration and contact tests were performed and their limited applicability for catalysis by bases with low solubility was shown. Li_2CO_3 showed the highest catalytic activity for the isomerization, resulting in 25% Fru yield in 10 minutes at 80 °C. The selectivity of the isomerization depends on the catalyst nature. The highest selectivity for Fru formation was observed in the presence of $MgCO_3$, giving rise to 27% Fru yield at 80 °C. $MgCO_3$ and MgO could be recycled without loss of activity.

Introduction

Isomerization of D-glucose (Glc) into D-fructose (Fru) is of utmost importance for the production of high fructose corn syrup (HFCS) in the food industry.[1,2] This reaction has attracted significant attention in recent years as a key transformation of cellulosic biomass into valuable products *via* platform chemicals.[3–9] Platform molecules derived from cellulosic biomass represent an attractive alternative for petroleum-based platform chemicals. Glucose obtained from cellulose can be transformed into highly valuable platform chemicals such as 5-hydroxymethylfurfural (5-HMF) or levulinic acid (LA), with fructose as the key intermediate.[10] In this regard, the development of chemo-catalysts for isomerization[11–13] is highly desired from an economic perspective. Recent efforts have predominantly focused on elaborating a solid catalyst aiming at its utilization in a continuous isomerization process, *e.g.* using a plug flow reactor[14] or a CSTR.[15] Solid bases[16] and solid Lewis acids[17] exhibit comparable catalytic activity for the isomerization though the Lewis acids catalyze co-formation of D-mannose in somewhat higher amounts. A broad range of solid bases exhibit catalytic activity for the isomerization, which includes MgO[14,18,19] and other alkaline earth metal (hydr)oxides,[20] MgO-doped ordered mesoporous carbon,[21] Mg–Al hydrotalcites,[14,15,18,22–30] Mg- or Ca-impregnated or exchanged zeolites,[31–35] attapulgite,[36,37] MgO–Nb phosphate,[38] Mg-doped carbon nitride,[39] Mg-containing titanosilicates,[40] $CaO–ZrO_2$,[41] $MgO–ZrO_2$,[42] MgO/biochar,[43] $CaO–Al_2O_3$,[44] CaO–MgO,[45] CaO/C,[46] alkaline earth metal titanates,[47] soluble amines[48–58] and N-containing solid catalysts,[50,51,54,55,59–63] silicates,[64] SiO_2 treated with ammonia,[65] zirconium carbonate,[66] ZrO_2 [67] and basic hybrid catalysts.[68] Nevertheless, establishing structure–activity and structure-selectivity correlations between the textural properties of materials and their catalytic performance remains challenging.[64] This hampers the knowledge-driven development of a catalyst for the isomerization and results in a rather trial-and-error approach to seeking a suitable material.

Recently, we utilized MgO, CaO, SrO, and $Ba(OH)_2$ as solid catalysts for Glc–Fru isomerization. Our results suggest that OH^- is generated *in situ* by partial dissolution of the materials as catalytically active species.[20] The oxides are readily transformed into hydroxides, and the latter release

[a] *Institute of Chemical, Environmental and Bioscience Engineering, TU Wien, Getreidemarkt 9, 1060 Vienna, Austria. E-mail: Irina.delidovich@tuwien.ac.at*
[b] *Chair of Heterogeneous Catalysis and Chemical Technology, Institute for Technical and Macromolecular Chemistry, RWTH Aachen University, Worringerweg 2, 52074 Aachen, Germany*

† Electronic supplementary information (ESI) available: Characterization of catalysts, results of catalytic, filtration, contact, and recycling tests. See DOI: **https://doi.org/10.1039/d2cy00551d**

This journal is © The Royal Society of Chemistry 2022

Open Access Article. Published on 04 May 2022. Downloaded on 10/16/2025 5:20:47 PM. This article is licensed under a Creative Commons Attribution-NonCommercial 3.0 Unported Licence.

hydroxide anions according to eqn (1):

$$M(OH)_2 \overset{H_2O}{\rightleftarrows} M^{2+} + 2OH^- \quad (1)$$

Along with alkaline earth metal (hydr)oxides, basic salts with low solubility represent another important class of solids, which are frequently utilized as catalysts for isomerization. For example, the catalytic activity of phosphates,[38] titanosilicates,[40] titanates,[47] silicates,[64] and carbonates[66] was reported.

In this work, we systematically explored basic salts with low solubility – carbonates and phosphates – to reveal the nature of catalytically active species and investigate the relationship between catalyst composition and catalytic performance. For this purpose, Li_2CO_3, $MgCO_3$, $CaCO_3$, $SrCO_3$, and $BaCO_3$ were utilized in this study. These materials generate hydroxide ions upon contact with the aqueous phase owing to partial dissolution according to eqn (2), followed by the protonation of carbonate anions in accordance with eqn (3).

$$M_2(CO_3)_n \overset{H_2O}{\rightleftarrows} 2M^{n+} + nCO_3^{2-} \quad (2)$$

$$CO_3^{2-} + H_2O \rightleftarrows HCO_3^- + OH^- \quad (3)$$

In addition, the catalytic properties of the phosphates with low solubility Li_3PO_4 and $Mg_3(PO_4)_2$ were investigated. These catalysts release OH^- species *via* a partial dissolution and protonation of the phosphate anion according to eqn (4) and (5).

$$M_3(PO_4)_n \overset{H_2O}{\rightleftarrows} 3M^{n+} + nPO_4^{3-} \quad (4)$$

$$PO_4^{3-} + H_2O \rightleftarrows HPO_4^{2-} + OH^- \quad (5)$$

Magnesium oxide MgO was used as a reference catalyst.

Experimental

Chemicals

All chemicals were used as received without further purification. MgO (>99.0%), D-glucose (≥99.5%), Li_2CO_3 (≥99.0%), $SrCO_3$ (≥99.0%), $CaCO_3$ (≥99.0%), $BaCO_3$ (≥99.0%), Dowex® 66 free base, and Amberlyst® 15 H-form were purchased from Sigma Aldrich. Li_3PO_4 (99.0%) was obtained from BLD Pharmatech Ltd. Na_2CO_3 (99.8%), acetone (99.8%), NaOH (99.5%), and $NaNO_3$ (99.5%) were supplied by Chemsolute. Anhydrous $MgCl_2$ (99.0%) was obtained from Alfa Aesar. Phosphoric acid (≥85 wt% H_2O) was purchased from Fluka. Ammonia solution (25.0%) was supplied by Supelco. Sulfuric acid (98.0%) was obtained from Merck. *n*-Tetradecane (99.5%) was purchased from J&K. $MgNO_3{\cdot}6H_2O$ (99.0%) was received from Fluka and $NaHCO_3$ (≥99.0%) by Roth. All solutions were prepared in distilled water.

Synthesis of $MgCO_3$

$MgCl_2$ (3.75 g, 39.3 mmol) was dissolved in 75 mL water and Na_2CO_3 (3.97 g, 37.5 mmol) was dissolved in 75 mL water. The product was obtained *via* precipitation by dropwise addition of the $MgCl_2$ solution to the Na_2CO_3 solution. The solution was added over a time period of 20 min. It is of utmost importance that the solution is added slowly at room temperature. A faster addition of the $MgCl_2$ solution can result in a change of the catalyst composition, which leads to a significantly lower pH_0 in the catalytic tests. The obtained white slurry was stirred for 1 h at RT. The white powder was filtered off and dried in a drying oven at 80 °C for 2 days. $Mg_5(CO_3)_4(OH)_2(H_2O)_4$ was obtained in a yield of 2.60 g (0.56 mmol, 72%). The structure was confirmed by XRD (ESI,† Fig. S3).

Synthesis of $Mg_3(PO_4)_2$

$Mg_3(PO_4)_2$ was synthesized according to the procedure described by Mousa *et al.*[69] $Mg(NO_3)_2{\cdot}6H_2O$ (12.82 g, 50 mmol, 1 eq.) and phosphoric acid (1.93 mL, 33.3 mmol, 0.6 eq.) were dissolved in H_2O (500 mL). The product was precipitated by dropwise addition of aqueous 3M NaOH solution (100 mL). After the precipitation, the white gel was allowed to stand overnight without stirring. The white slurry was filtered and washed with H_2O. The white precipitate was dried in air overnight and then calcined for 6 h at 850 °C (temp ramp 10 K min^{-1}). $Mg_3(PO_4)_2$ was obtained as a white powder (3.0 g, 11.4 mmol, 69%). The structure was confirmed by XRD (ESI,† Fig. S1).

Catalyst characterization

The tested catalysts were explored by N_2 physisorption at −196 °C using a Quadrasorb SI automated surface area and pore size analyzer. The samples were degassed under vacuum prior to the analysis at 150 °C for 2–3 h using a Quartrachrome Instruments FloVac degasser. The specific surface areas S_{BET} were determined using the BET model (Brunauer–Emmett–Teller) in a range of $0.05 \leq p/p_0 \leq 0.2$. The total pore volumes were determined by the N_2 adsorbed at the highest relative pressure point, p/p_0 = 0.95–0.98.

The solids were characterized by X-ray diffraction analysis (XRD) without any pre-treatment. A Bruker D2 Phase diffractometer with a CuKα X-ray tube was used for the measurements. The tube voltage was 40 kV, and diffractometer patterns were collected in the 10–90 °C 2θ range with 0.02° intervals and a step time of 1 s.

Isomerization reaction

A 10 wt% D-glucose solution (40 mL) was heated in a 50 mL two-neck flask equipped with a reflux condenser for the isomerization of D-glucose to D-fructose. The reaction was started by the addition of the appropriate amount of catalyst. The samples (2.5 mL) were taken using a syringe at different time intervals, filtered through a syringe filter (CHROMAFIL,

Open Access Article. Published on 04 May 2022. Downloaded on 10/16/2025 5:20:47 PM. This article is licensed under a Creative Commons Attribution-NonCommercial 3.0 Unported Licence.

medium polar, 0.25 μm), and cooled in an ice bath to stop the reaction. The pH values were measured with a pH-electrode (Hannah instruments® HI1230).

Filtration and contact tests

For the filtration tests, a 10 wt% glucose solution (40 mL) was heated in a 50 mL two-neck flask until 60 or 80 °C. The reaction was started by adding the catalyst to the heated solution. At a low conversion of 4–20%, the catalyst was removed by filtration through a syringe filter (CHROMAFIL, PA-20/25, 0.25 μm). The solution was allowed to further react at the corresponding temperature.

For the contact tests, the catalyst was stirred in distilled water (40 mL) for 30 min at 60 or 80 °C. The catalyst was filtered off through a syringe filter (CHROMAFIL, PA-20/25, 0.25 μm), and the solution was again heated to the desired temperature. As the reaction temperature was reached, 10 wt% glucose was added to the solution, and samples were taken at different time intervals and cooled in an ice bath to stop the reaction. The pH of the solution was measured with a pH-electrode (Hannah instruments® HI1230).

Recycling

Recycling tests with MgO and $MgCO_3$ were performed. After the isomerization experiment, the catalyst was washed several times with deionized water and acetone. The catalyst was dried for two days in the drying oven at 80 °C. MgO was also calcined for 3 h at 500 °C (5 K min^{-1}).

Analysis of the product mixture

The concentrations of D-glucose and D-fructose were determined by GC analysis. Prior to measurement, the samples were 10-fold diluted with distilled water. Ionic species were removed by ion exchange resins. Therefore, at room temperature, the diluted samples were stirred for 0.5 h with 400 mg Amberlyst® 15 in the H^+-form. Next, the samples were allowed to stir for 1 h with 1000 mg of Dowex® 66 free base at room temperature. The treatment with the ion exchange resins was repeated twice. Importantly, no adsorption of Glc or Fru onto Amberlyst® 15 in the H^+-form takes place during the treatment. About 6–11% of the saccharides were adsorbed on Dowex® 66 free base with approximately the same amounts for Glc and Fru.

After treatment with the ion exchange resins, samples were analyzed according to the modified GC analysis method proposed by Ekeberg *et al.*[20,70] In this procedure, the aldoses and ketoses are converted into their isopropylidene derivatives by derivatization. Therefore, 1 mL of deionized samples was freeze-dried in a desiccator, yielding saccharides as solids. *n*-Tetradecane (15 μL) was added as an internal standard. The derivatization reagent was prepared by the addition of sulfuric acid (98%, 1.76 mL) to acetone (100 mL). The derivatization agent (2.5 mL) was added to the dried sample and shaken for 2.5 h at a shaking plate. Then, $NaHCO_3$ (800 mg) was added, and the samples were neutralized for 1 h. After neutralization, the samples were filtered through a syringe filter (CHROMAFIL, PTFE-20/25, 0.25 μm).

Analysis by GC was performed with an HP 6890 gas chromatograph, equipped with a Machery-Nagel Optima 17-MS column (30 m × 0.25 mm). For the measurement, the FID and the temperature programmed detector were combined upon increasing the temperature from 80 to 250 °C with a heating rate of 12 K min^{-1}. Based on the areas of the derivatives in combination with the peak area of the standard, the concentrations of monosaccharides were determined. The signal of *n*-tetradecane was obtained at 6.3 min. The peak at 10.6 min corresponds to D-glucose. D-Fructose showed two signals at 10.1 and 10.7 min, and the concentration was calculated by combining the areas of both peaks.

Results and discussion

Kinetic study of the base-catalyzed isomerization reaction

The following solid bases were purchased: MgO, Li_2CO_3, $CaCO_3$, $SrCO_3$, $BaCO_3$, and Li_3PO_4. $MgCO_3$ and $Mg_3(PO_4)_2$ were synthesized. The materials were characterized *via* X-ray diffraction and low temperature physisorption of N_2. The results of the characterization are presented in the ESI† (Fig. S1–S4 and Table S1). Upon dispersion in water, the materials release hydroxide anions according to eqn (1)–(5). In this regard, the high alkalinity of the aqueous phase is expected for the materials with large solubility product constants (K_{sp}).[32] The highest concentration of the OH^- anions in the liquid phase upon contact with the materials can be predicted from the thermodynamic data, *i.e.* the solubility product constants and protonation constants. However, low solid-to-liquid loadings can lead to undersaturated solutions.[10,33] In order to obtain the liquid phases with the maximum alkalinity for each material, we prepared suspensions upon a systematic variation of solid-to-liquid ratios and measured the pH of the aqueous phase. We used either water or 10 wt% aqueous Glc solution as the liquid phase. The pH values of the Glc solution were always somewhat lower than those of pure water due to the acidity of Glc.[71] The results are shown in Fig. S5.† Finally, we found the saturation conditions corresponding to the highest alkalinity for each material. As expected, the pH values correlated with the K_{sp} in the range from pH 7.8 for $CaCO_3$ ($K_{sp} = 3.36 \times 10^{-9}$) to pH 10.6 for Li_2CO_3 ($K_{sp} = 8.15 \times 10^{-4}$).[72] Table 1 lists the pH values of the Glc slurries in the presence of the materials.

According to our knowledge, Li_2CO_3, $MgCO_3$, Li_3PO_4, $SrCO_3$, $CaCO_3$, $BaCO_3$, and $Mg_3(PO_4)_2$ have not been examined as catalysts for Glc isomerization yet. We tested the materials for the isomerization using the solid-to-liquid ratios corresponding to the saturation conditions (Table S2†) in a batch reactor at 60 or 80 °C. Formation of Fru as the main product was observed. D-Mannose and D-allulose were detected in minor amounts for highly active catalysts, though

 This journal is © The Royal Society of Chemistry 2022

Open Access Article. Published on 04 May 2022. Downloaded on 10/16/2025 5:20:47 PM.
This article is licensed under a Creative Commons Attribution-NonCommercial 3.0 Unported Licence.

Table 1 Results of the catalytic tests. Reaction conditions: 40 mL 10 wt% Glc solution, 500 rpm, pH_0 were measured directly prior to the reaction

Entry	Catalyst	Catalyst loading, g mL^{-1}	T, °C	pH_0	t_{ind},[a] h	$<S_{15-30}>$,[b] %	Maximum Fru yields			
							Y_{max},[c] %	X,[d] %	Time,[e] h	[M^{n+}],[f] mM
1	Li_2CO_3	0.022	60	10.6	0.08	56	21	45	2	280
2	Li_2CO_3	0.022	80	10.5	0.02	64	25	48	0.15	230
3[g]	MgO	0.054	40	10.2	0.75	50	10	20	24	5
4	MgO	0.004	60	10.2	0.5	63	22	44	22	48
5	MgO	0.004	80	10.2	0.05	65	25	55	5	57
6	$MgCO_3$	0.042	60	9.6	2	77	27	24	30	16
7	$MgCO_3$	0.042	80	9.8	0.08	72	27	36	5	16
8	Li_3PO_4	0.0116	60	9.7	1	76	14	16	26	65
9	Li_3PO_4	0.0116	80	9.7	0.08	77	17	20	3	20
10	$SrCO_3$	0.007	80	8.1	2	47	11	22	30	7
11	$BaCO_3$	0.010	80	8.1	1	40	7	16	30	26
12	$Mg_3(PO_4)_2$	0.053	80	7.9	1.5	45	4	9	22	11
13	$CaCO_3$	0.010	80	7.8	2	71	11	16	26	9

[a] Induction time: for this time lapse, no Fru formation occurred. [b] An average selectivity for the conversion range of 15 to 30%. [c] Maximum yield of Fru. [d] Glc conversion, at which the maximum Fru yield was observed. [e] Reaction time, at which the maximum yield of Fru was detected. [f] Concentration of the leached metal in the solution. [g] Previously reported data.[20]

the yield of either did not exceed 3%. During the catalytic experiments, the pH values were decreasing constantly owing to the formation of acidic by-products. The pH value is mostly affected by the formation of lactic acid which was detected in the presence of earth alkaline metal oxides. Minor amounts of glycolic acid were also observed.[15,20] In addition, oxidation of enediol species with atmospheric oxygen cannot be excluded. We measured the initial rates of Fru formation to estimate its dependency on the concentration of OH^- anions. Noteworthily, materials with low basicity, such as $CaCO_3$, $BaCO_3$, $Mg_3(PO_4)_2$, and $SrCO_3$, showed no catalytic activity at 60 °C even after a few hours of incubation.

The isomerization of Glc in the presence of bases occurs *via* deprotonation of the substrate, followed by formation of an enediol anion intermediate.[73] Since the concentration of the highly reactive enediol (ED) anion can hardly be measured, it is usually omitted in the kinetic modeling. Fig. 1 shows the simplest reaction network used to describe the reaction kinetics.[20,71]

Based on this network, Kooyman *et al.* proposed the following equation for the initial reaction rate of Fru formation:[71]

$$r_0 \approx \frac{d[\mathrm{Fru}]}{\mathrm{d}t} = -k_1 \cdot \frac{K_{\mathrm{Glc}} \cdot [\mathrm{OH}^-]}{K_{\mathrm{Glc}} \cdot [\mathrm{OH}^-] + 1} \cdot [\mathrm{Glc}] \quad (6)$$

where k_1 is an apparent rate constant and K_{Glc} stands for the dissociation constant of Glc. A dependence of the initial reaction rate on the concentration of the hydroxide ions can be expressed in the logarithmic form according to eqn (7):

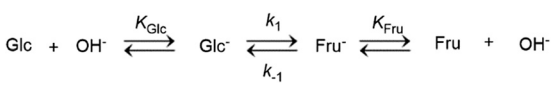

Fig. 1 Kinetic reaction network proposed by Kooyman *et al.*[71]

$$\ln r_0 = \ln \frac{K_{\mathrm{Glc}} \cdot [\mathrm{OH}^-]}{K_{\mathrm{Glc}} \cdot [\mathrm{OH}^-] + 1} + \mathrm{const.} \quad (7)$$

This expression was shown to hold true for NaOH as the catalyst.[71] We recently demonstrated that the dependency of r_0 on [OH^-] in the presence of MgO, CaO, SrO, and $Ba(OH)_2$ also follows eqn (7). Based on this, we concluded that OH^- ions generated *in situ via* partial dissolution according to eqn (1) are catalytically active species for catalysis by alkaline earth metal hydr(oxides).[20] In this work, we also used eqn (7) to obtain a dependency of $r_{0,Fru}$ on the concentration of OH^- in the presence of the basic salts with low solubility. We considered changes of the pH values during the reaction and used the average values of [OH^-] for the initial time lapse. Fig. 2 shows the obtained plots. For both 60 and 80 °C, linear dependencies were observed. Moreover, linearization coefficients of (0.9 ± 0.1) at 60 °C and (0.8 ± 0.04) at 80 °C were very close to unity, as expected from eqn (7). The results for the reference catalyst MgO are also in agreement with those for the basic salts with low solubility. Based on these data, we conclude that the OH^- anions released *via* partial dissolution of the materials followed by protonation (eqn (2)–(5)) are the catalytically active species. The isomerization of Glc is catalyzed thus homogeneously.

This conclusion is further supported by the results obtained in the presence of Li_2CO_3 with different loadings of the catalyst. We performed the isomerization of Glc catalyzed by Li_2CO_3 using 0.008, 0.012, or 0.016 mol of the material. Under these conditions, the pH_0 value was 10.5 in all three cases, and the aqueous phase remained saturated. The same initial reaction rate was observed in all three experiments (Fig. S6†). This indicates that the reaction rate is dependent on the pH value rather than on the amount (*i.e.* the surface area) of the materials, supporting the homogeneous nature of the catalysis.[20]

Open Access Article. Published on 04 May 2022. Downloaded on 10/16/2025 5:20:47 PM.
This article is licensed under a Creative Commons Attribution-NonCommercial 3.0 Unported Licence.

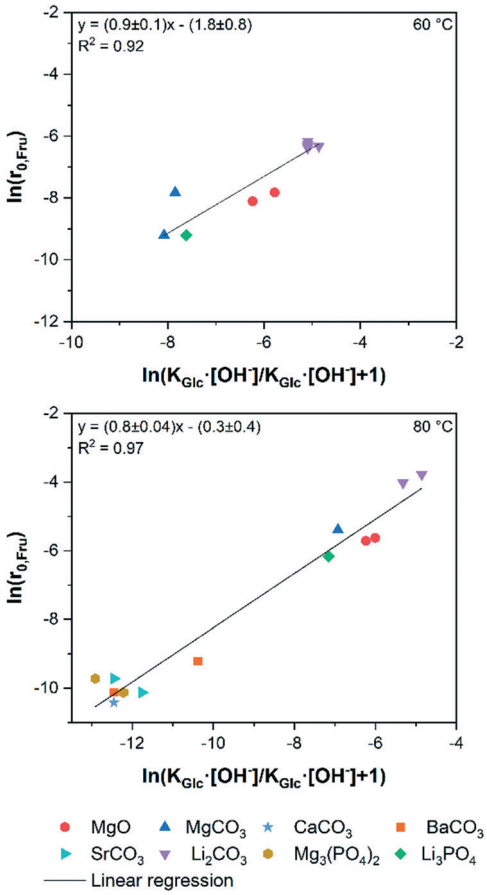

Fig. 2 Initial rates of Glc isomerization into Fru plotted in linearized coordinates according to eqn (7) at 60 and 80 °C. Reaction conditions: 40 mL 10 wt% Glc aqueous solution, 500 rpm.

Structure–selectivity relations

For all the catalysts, the induction period for Fru formation was observed. De Wit *et al.* explained this induction period by the accumulation of ED anions until the pseudo-steady state concentration of the latter is reached.[73] The induction time has been previously published for other base catalysts, *i.e.* KOH,[73] Mg–Al hydrotalcite,[28] phosphates,[74] MgNa-ZSM-5,[34] and alkaline earth metal (hydr)oxides.[20] Table 1 lists the durations of the induction period for different catalysts and temperatures. Apparently, high alkalinity along with high temperature facilitates reduction of the induction period. Thus, catalysts with low activity, generating low alkalinity, such as $SrCO_3$, $BaCO_3$, $Mg_3(PO_4)_2$, or $CaCO_3$, exhibit 1–2 hours induction period, whereas accumulation of Fru was detected in the presence of Li_2CO_3 at 80 °C in only 1 minute. For practical application, the short induction time is beneficial.

Interestingly, selectivity for Fru is typically low for the conversion below *ca.* 15%. The substrate predominantly decomposes during the initial period of time. Once the concentration of ED attains its pseudo-steady state, the reaction diverts from the destruction to the isomerization.[20] At Glc conversion over 30%, selectivity for Fru drops again due to decomposition processes. Thus, the highest selectivity for Fru formation is typically reached for 15–30% Glc conversion. The average selectivities for the conversion range of 15–30% were denoted as $\langle S_{15-30}\rangle$ and are listed in Table 1. For all the catalysts, $\langle S_{15-30}\rangle$ was somewhat higher at 80 °C than at 60 °C.

In the previous section, we showed that OH^- anions catalyze the isomerization, and the reaction rate is determined by the ability to generate alkalinity owing to partial dissolution and protonation. Here, we would like to discuss the relationships between the selectivity and structure of the tested catalysts. For this purpose, we tentatively organize the materials in three groups, namely:

- materials with high alkalinity Li_2CO_3 and MgO, which generate a pH_0 of 10.2–10.5;

- materials with medium alkalinity $MgCO_3$ and Li_3PO_4, generating a pH_0 of *ca.* 9.7;

- materials with low alkalinity $SrCO_3$, $CaCO_3$, $BaCO_3$, and $Mg_3(PO_4)_2$, generating a pH_0 of *ca.* 8.

Li_2CO_3 and MgO induce high pH values in the range of 10.2–10.5 catalyzing the isomerization. Fig. 3 shows the results for catalysis by Li_2CO_3 and MgO. Li_2CO_3 is the most catalytically active material generating the highest pH value. A Fru yield of *ca.* 25% was obtained in the presence of Li_2CO_3 in only 10 minutes at 80 °C. However, Li_2CO_3 exhibits the highest leaching compared to the other catalysts (Table 1). In general, Li_2CO_3 and MgO showed similar selectivity–conversion curves at 60 and 80 °C (Fig. 3 and S15 and S16). The same maximum Fru concentration was obtained in the presence of Li_2CO_3 and MgO.

$MgCO_3$ and Li_3PO_4 are designated here as "medium-alkaline materials", generating a pH_0 of *ca.* 9.5–9.7. $MgCO_3$ catalyzes Fru formation at a very high selectivity up to *ca.* 90%, also at a low conversion of a few percentages. This dramatically differs from other catalysts, such as Li_2CO_3 and MgO (Fig. 3) or Li_3PO_4 (Fig. 4). Noteworthily, this result was reproducible. The high selectivity for Fru formation in the presence of $MgCO_3$ resembles the high selectivities for Fru reported for catalysis by Mg–Al hydrotalcites in the carbonate form.[15,22,24,26,32] Interestingly, carbonate as the counter-anion seems to play a crucial role in catalysis by hydrotalcites.[26]

This study also suggests a combination of Mg^{2+} and CO_3^{2-} counterparts as the key for the outstanding selectivity. Catalysts bearing only carbonate (*e.g.* Li_2CO_3) or solely magnesium (*e.g.* MgO) do not exhibit such favorable selectivity–conversion curves. As a result, the highest Fru yield of 27% was obtained in this study in the presence of $MgCO_3$ at 80 °C. The reason for the high Fru selectivity in the presence of the catalyst bearing both carbonate and magnesium remains unknown. It was proposed that Mg^{2+} ions interact with carbonate and hydrocarbonate anions in aqueous solution.[77] These complexes can probably react with the intermediates during the isomerization, *e.g.* with the ED anion. Moreover, coordination of an ED intermediate to Mg^{2+} ions was proposed for enzymatic catalysis.[78] Further experimental work is required to uncover the reason for the

 This journal is © The Royal Society of Chemistry 2022

Open Access Article. Published on 04 May 2022. Downloaded on 10/16/2025 5:20:47 PM.
This article is licensed under a Creative Commons Attribution-NonCommercial 3.0 Unported Licence.

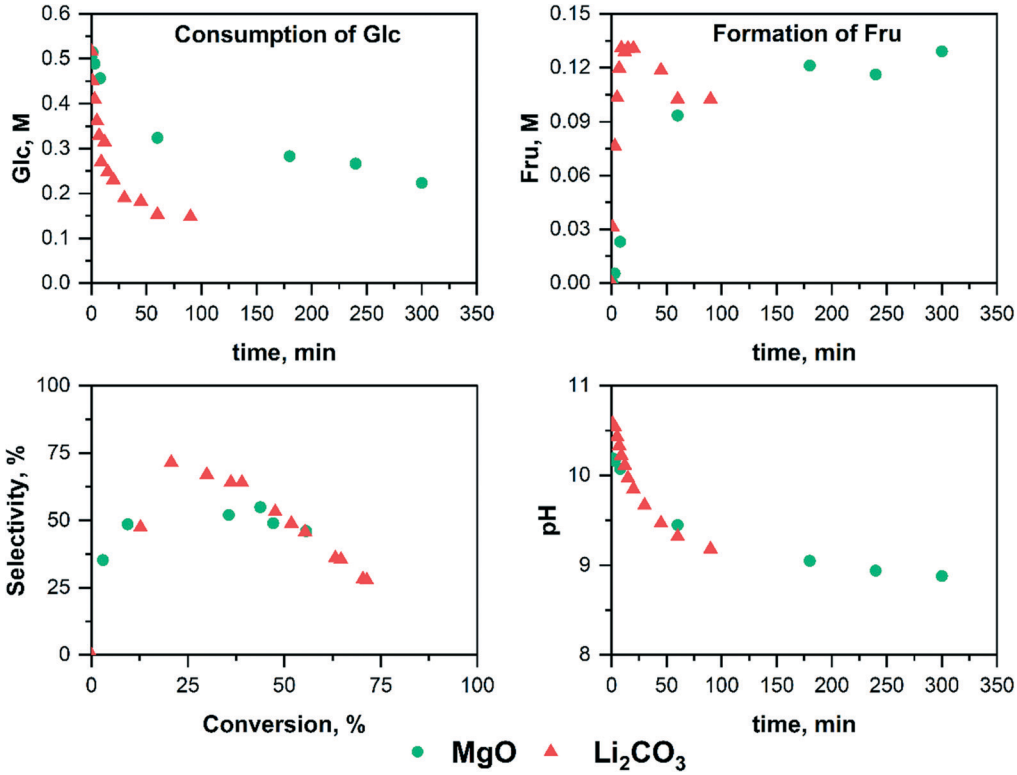

Fig. 3 Concentrations of Glc and Fru, selectivity–conversion curves, and pH values during the conversion of D-glucose in the presence of MgO (circles) and Li_2CO_3 (triangles) at 80 °C. Reaction conditions: 40 mL 10 wt% Glc aqueous solution, 4 mmol MgO, 12 mmol Li_2CO_3, 80 °C, 500 rpm.

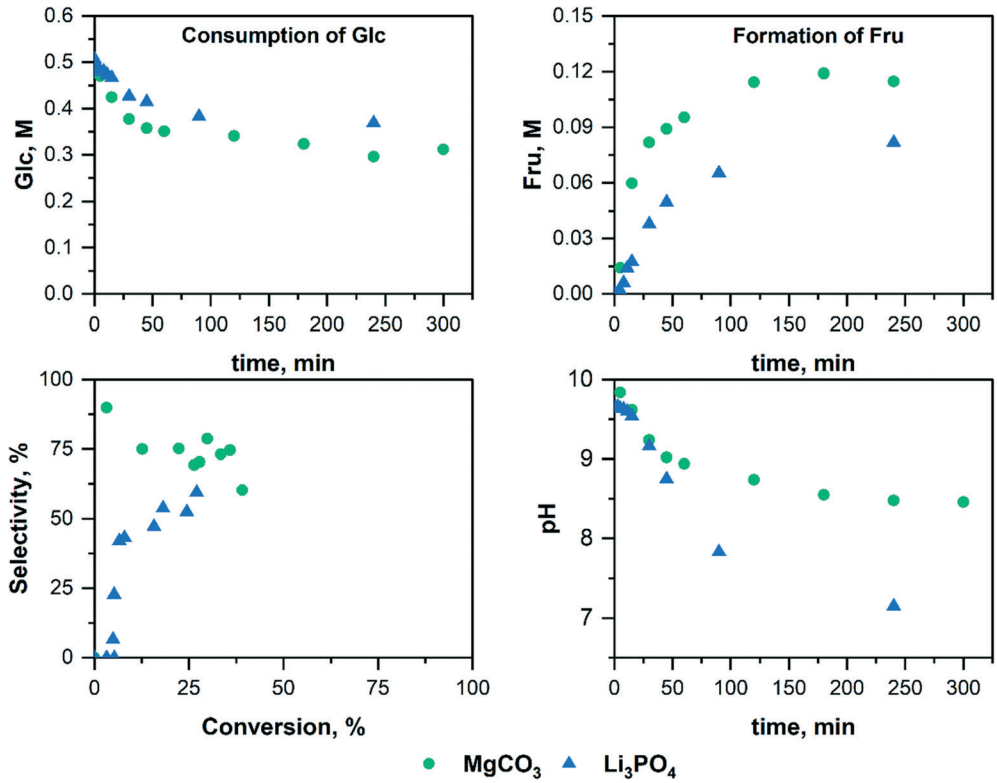

Fig. 4 Concentrations of Glc and Fru, selectivity–conversion curves, and pH values during the conversion of D-glucose in the presence of $MgCO_3$ (circles) and Li_3PO_4 (triangles) at 80 °C. Reaction conditions: 40 mL 10 wt% Glc aqueous solution, 4 mmol $MgCO_3$, 4 mmol Li_3PO_4, 500 rpm.

Open Access Article. Published on 04 May 2022. Downloaded on 10/16/2025 5:20:47 PM.
This article is licensed under a Creative Commons Attribution-NonCommercial 3.0 Unported Licence.

high selectivity for Fru formation in the presence of magnesium-carbonate containing materials. Contrary to magnesium carbonate, Li_3PO_4 exhibits worse selectivity for Fru formation, especially at low conversions of the substrate (Fig. 4 and S17†). The pH value drops in the presence of Li_3PO_4 significantly quicker than over $MgCO_3$ probably due to the formation of acidic by-products in a higher amount. This dramatic difference for catalysis by $MgCO_3$ and Li_3PO_4 points to the great importance reaction selectivity.

The effect of the leached Li^+ ions on the isomerization of Glc to Fru has not been examined. Based on the results of Angyal *et al.*, complexation of Li^+ with saccharides is unlikely. They reported no complexation of D-allose with LiCl,[75] and, in general, concluded that the cations smaller than Ca^{2+} (1.05 nm radius) do not tend to complex with polyols.[76] The radius of Li^+ is 0.76 nm. Nevertheless, formation of labile complexes between Li^+ and anionic intermediates can potentially impact the isomerization rate.

Filtration and contact tests

The results of the kinetic study strongly suggest that the isomerization of D-glucose to D-fructose is homogeneously catalyzed by OH^- ions in solution. The hydroxide anions are generated by partial dissolution of the catalyst and protonation of the anions. These hydroxide anions catalyze the isomerization reaction according to the reaction mechanism proposed by De Wit *et al.*[73] In this mechanism, OH^- ions deprotonate Glc followed by an intramolecular proton abstraction. Besides the kinetic study, filtration and contact tests present a potent and straightforward tool for the exploration of the catalytically active species. In filtration tests, the catalyst is removed at low conversion, and the filtrate is further incubated. In contact tests, the catalyst is stirred in water and removed, and then D-glucose is added. Filtration and contact tests were already performed for the isomerization of D-glucose in the presence of alkaline earth metal (hydr)oxides. The authors concluded that it might be challenging to distinguish between truly heterogeneous catalysis and catalysis by *in situ* generated OH^- based on the filtration tests – especially for the low-soluble catalysts generating hydroxide ions at low concentration.[20]

Here, we performed filtration tests (Fig. 5) and contact tests (Fig. S22†) for the isomerization in the presence of Li_3PO_4 and Li_2CO_3. As a reference, a filtration test for MgO was also performed. The results of the filtration test for MgO at 80 °C are similar to the results of the tests performed at 40 °C.[20] After removing the catalyst, the reaction rate significantly decreased as well as the pH of the solution (Fig. 5). For the filtration test with Li_3PO_4, less Fru is formed after removal of the catalyst. The pH of the solution also decreases but the difference is not as significant as for MgO (Fig. 5). Upon catalyst removal, the source for the generation of the active species is also removed. Consequently, the pH decreases due to the missing *in situ* formation of OH^- ions, and the hydroxide anions are partially neutralized by acidic by-products. The leaching results of the catalysts also confirm this reaction mechanism during the isomerization reaction

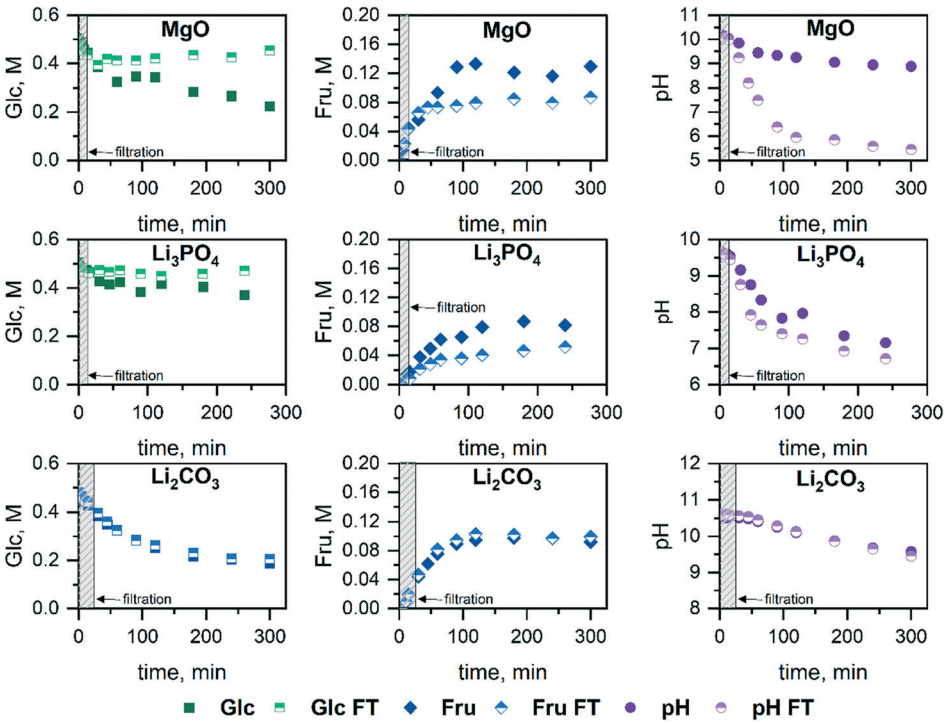

Fig. 5 Filtration tests of the conversion of D-glucose in the presence of MgO, Li_3PO_4, and Li_2CO_3. Reaction conditions: 40 mL 10 wt% aqueous solution; MgO (80 °C), 4 mmol Li_3PO_4 (80 °C), 12 mmol Li_2CO_3 (60 °C), 500 rpm.

Open Access Article. Published on 04 May 2022. Downloaded on 10/16/2025 5:20:47 PM.
This article is licensed under a Creative Commons Attribution-NonCommercial 3.0 Unported Licence.

(Fig. S20 and S21†). The leaching *vs.* time plots for MgO and Li_3PO_4 showed that the metal contents increased during the dissolution reaction, accompanied by *in situ* generation of OH^- species. For the contact tests with MgO (ref. 20) and Li_3PO_4, the same results as for the filtration tests were found. In the absence of the catalyst, a significant decrease of the reaction rate of the isomerization could be observed.

The results of the filtration and contact tests for Li_2CO_3 are consistent with the results of the kinetic data. After removing the catalyst, D-glucose consumption and D-fructose formation were observed. According to the metal leaching results (Fig. S20 and S21†), the OH^- ions are directly released into the aqueous solution after immersion of the catalyst into water and do not significantly increase during the reaction. Fru formation could also be observed in the absence of the catalyst through the prior generation of the OH^- species in aqueous solution by stirring of the catalyst in water. The filtration and contact tests of Li_2CO_3 correspond to the results of $Ba(OH)_2$ obtained by Drabo *et al.*[20] The results of this study are in excellent agreement with the previously reported data on catalysis by alkaline earth metal (hydr) oxides. For the materials with higher solubility, such as Li_2CO_3 or previously reported $Ba(OH)_2$, OH^- and carbonate ions are generated at a high concentration (pH_0 10.6 for Li_2CO_3) directly upon the catalyst immersion into an aqueous phase. Due to a high concentration of hydroxide species, deactivation owing to neutralization of OH^- by acidic by-products is negligible. In this case, filtration and contact tests clearly indicate homogeneous catalysis by leached species.

The situation for Li_3PO_4 is more complex (pH_0 9.7). Since this material is significantly less soluble than Li_2CO_3, lithium phosphate constantly generates OH^- during the reaction owing to dissolution and protonation of phosphate anion. Importantly, a contact test with Li_3PO_4 shows literally no formation of Fru (Fig. S22†), whereas a significant deceleration of the isomerization was observed in the filtration test. The same results were obtained for MgO (Fig. 5).[20] Such results are often interpreted as "heterogeneous" or "partially heterogeneous" catalysis.[13] This study provides evidence that the results of filtration and contact tests must be interpreted with caution. Investigation of the reaction kinetics as well as monitoring of the leached species during the reaction is of great importance for drawing valid conclusions.

Recycling

Benefits of solid basic catalysts for Glc–Fru isomerization include the simple recycling of the catalyst by filtration. In the literature, several recycling tests of MgO for the isomerization of D-glucose to D-fructose were already performed and showed a possibility to reuse MgO.[19] Table 2 shows the results of the recycling tests for the isomerization of D-glucose with MgO and $MgCO_3$. The recycling tests for MgO were performed according to the procedure by Marianou *et al.*[19] The catalyst was either washed or calcined after the first run. After the 1st cycle, the color of MgO changed from white to dark orange, indicating the adsorption of dehydrated by-products (Fig. S23 and S24†). In addition, the XRD data showed that after the first cycle, the composition of the material changed, containing a higher amount of $Mg(OH)_2$. After calcination at 500 °C, the catalyst could be regenerated with MgO as the main phase. The calcined catalyst could generate the same pH_0 in the 2nd run, leading to approximately the same initial reaction rate for fructose formation (entries 1 and 2 in Table 2). We made an attempt to avoid calcination of MgO and perform regeneration of MgO by washing of used MgO with acetone to remove adsorbed organic species (entries 3 and 4, Table 2). The pH value after the first run for the washed MgO is about 0.3 lower compared to the pH generated by the fresh MgO, resulting in a somewhat lower $r_{0,Fru}$ though a comparable yield of Fru. These results suggest that the calcination of MgO after the 1st cycle gives somewhat better results.

For the isomerization of D-glucose with $MgCO_3$, the results show that washing with acetone presents a suitable method for catalyst regeneration (entries 5 and 6, Table 2). The same initial reaction rates as well as pH values could be obtained for fresh and recycled $MgCO_3$. XRD data also confirmed that there are no structural changes after the 1st and 2nd cycle of the isomerization. Thus, $MgCO_3$ could be successfully separated and reused for the isomerization of Glc to Fru.

$MgCO_3$ exhibits promising catalytic performance, the highest activity and selectivity for Fru among the tested catalysts. Nonetheless, leaching of Mg^{2+} poses a question on the long-term stability of this catalyst. Calculations considering the concentration of the leached Mg^{2+} (16 mM, entries 6 and 7 in Table 1) as well as a catalyst loading of

Table 2 Results of the recycling tests

Entry	Catalyst	Cycle	T, °C	n, mmol	pH_0	r_0, mmol L^{-1} min^{-1}	Y_{max},[a] %	X_{max},[b] %	Time,[c] h
1	MgO	1	80	25	9.9	2.08	15	49	2
2	MgO calcined[d]	2	80	25	10.0	2.20	14	53	2
3	MgO	1	60	4	10.3	0.97	23	28	5
4	MgO washed[e]	2	60	4	10.0	0.53	21	18	5
5	$MgCO_3$	1	80	4	9.5	2.07	26	30	4
6	$MgCO_3$ washed[e]	2	80	4	9.4	2.07	27	34	4

[a] Maximum yield of Fru. [b] Glc conversion, at which the maximum Fru yield was observed. [c] Reaction time, at which the maximum yield of Fru was detected. [d] Catalyst calcined after the 1st cycle. [e] Catalyst washed with water + acetone and dried after the 1st cycle.

Open Access Article. Published on 04 May 2022. Downloaded on 10/16/2025 5:20:47 PM.
This article is licensed under a Creative Commons Attribution-NonCommercial 3.0 Unported Licence.

0.042 g mL^{-1} allow us to roughly assess the applicability of the catalyst for 28 cycles. In future research, recovery of the leached Mg^{2+} from the reaction solution and recycling of the metal for catalyst synthesis should be addressed.

Conclusion

In this study, we propose a series of basic salts with low solubility as catalysts for Glc isomerization into Fru and systematically investigated their catalytic performance. We focused on the crucial parameters such as catalytic activity and reaction selectivity. Li_2CO_3, $MgCO_3$, Li_3PO_4, $SrCO_3$, $CaCO_3$, $BaCO_3$, and $Mg_3(PO_4)_2$ were tested with MgO as the reference catalyst. The dependency of the initial reaction rate on the pH_0 strongly suggests hydroxide ions released by partial dissolution and protonation as catalytically active species. Thus, the rate of Glc isomerization in the presence of a low-soluble base can be predicted in a straightforward way based on the pH_0 value.

The selectivity of Fru formation depends strongly on the temperature and nature of the catalyst. The most promising results were obtained for $MgCO_3$. Based on our data, a synergistic effect of magnesium and carbonate species facilitating the high selectivity of Fru formation can be concluded. Despite leaching of Mg^{2+}, $MgCO_3$ can be recycled.

The results of filtration and contact tests can be misleading, especially for moderately soluble catalysts. These materials generate OH^- as catalytically active species in low concentrations. These diluted bases tend to quickly deactivate *via* neutralization with acidic by-products leading to incorrect conclusions on the contribution of homogeneous and heterogeneous catalysis.

Author contributions

VT: conceptualization, formal analysis, methodology, investigation, visualization, resources, validation, writing – original draft and writing – review & editing; ID: conceptualization, methodology, supervision, validation, funding acquisition, writing – original draft and writing – review & editing.

Conflicts of interest

There are no conflicts to declare.

Acknowledgements

We thank Prof. Dr. Regina Palkovits for valuable discussion, Noah Avraham and Jens Heller for HPLC and XRD measurements; and Elke Biener, Hannelore Eschmann and Heike Fickers-Bolz for performing GC measurements. We gratefully acknowledge financial support by the DFG (Deutsche Forschungsgemeinschaft, Project number 397970309). This work partly contributed to the Cluster of Excellence "The Fuel Science Center", which is funded by the Deutsche Forschungsgemeinschaft (DFG, German Research Foundation) under Germany's Excellence Strategy - Exzellenzcluster 2186 "The Fuel Science Center" (ID: 390919832).

Notes and references

1 L. M. Hanover and J. S. White, *Am. J. Clin. Nutr.*, 1993, **58**, 724S–732S.
2 K. Parker, M. Salas and V. C. Nwosu, *Biotechnol. Mol. Biol. Rev.*, 2010, **5**, 71–78.
3 I. Delidovich, P. J. Hausoul, L. Deng, R. Pfützenreuter, M. Rose and R. Palkovits, *Chem. Rev.*, 2016, **116**, 1540–1599.
4 I. Delidovich, K. Leonhard and R. Palkovits, *Energy Environ. Sci.*, 2014, **7**, 2803–2830.
5 R. De Clercq, M. Dusselier and B. Sels, *Green Chem.*, 2017, **19**, 5012–5040.
6 S. Shylesh, A. A. Gokhale, C. R. Ho and A. T. Bell, *Acc. Chem. Res.*, 2017, **50**, 2589–2597.
7 C. Chatterjee, F. Pong and A. Sen, *Green Chem.*, 2015, **17**, 40–71.
8 F. A. Kucherov, L. V. Romashov, K. I. Galkin and V. P. Ananikov, *ACS Sustainable Chem. Eng.*, 2018, **6**, 8064–8092.
9 R. A. Sheldon, *Curr. Opin. Green Sustainable Chem.*, 2018, **14**, 89–95.
10 A. Guleria, G. Kumari and S. Saravanamurugan, in *Biomass, Biofuels, Biochemicals*, Elsevier, 2020, pp. 433–457.
11 I. Delidovich and R. Palkovits, *ChemSusChem*, 2016, **9**, 547.
12 H. Li, S. Yang, S. Saravanamurugan and A. Riisager, *ACS Catal.*, 2017, **7**, 3010–3029.
13 I. Delidovich, *Curr. Opin. Green Sustainable Chem.*, 2021, **27**, 100414.
14 S. Souzanchi, L. Nazari, K. T. V. Rao, Z. Yuan, Z. Tan and C. C. Xu, *Catal. Today*, 2019, **319**, 76–83.
15 I. Delidovich and R. Palkovits, *Catal. Sci. Technol.*, 2014, **4**, 4322–4329.
16 C. Moreau, R. Durand, A. Roux and D. Tichit, *Appl. Catal., A*, 2000, **193**, 257–264.
17 M. Moliner, Y. Román-Leshkov and M. E. Davis, *Proc. Natl. Acad. Sci. U. S. A.*, 2010, **107**, 6164–6168.
18 D. Y. Murzin, E. V. Murzina, A. Aho, M. A. Kazakova, A. G. Selyutin, D. Kubicka, V. L. Kuznetsov and I. L. Simakova, *Catal. Sci. Technol.*, 2017, **7**, 5321–5331.
19 A. A. Marianou, C. M. Michailof, A. Pineda, E. F. Iliopoulou, K. S. Triantafyllidis and A. A. Lappas, *ChemCatChem*, 2016, **8**, 1100–1110.
20 P. Drabo, M. Fischer, V. Toussaint, F. Flecken, R. Palkovits and I. Delidovich, *J. Catal.*, 2021, **402**, 315–324.
21 J. Fu, F. Shen, X. Liu and X. Qi, *Green Energy Environ.*, 2021, DOI: **10.1016/j.gee.2021.11.010**.
22 I. Delidovich and R. Palkovits, *J. Catal.*, 2015, **327**, 1–9.
23 J. Lecomte, A. Finiels and C. Moreau, *Starch/Staerke*, 2002, **54**, 75–79.
24 G. Lee, Y. Jeong, A. Takagaki and J. C. Jung, *J. Mol. Catal.*, 2014, **393**, 289–295.
25 S. Yu, E. Kim, S. Park, I. K. Song and J. C. Jung, *Catal. Commun.*, 2012, **29**, 63–67.

 This journal is © The Royal Society of Chemistry 2022

Open Access Article. Published on 04 May 2022. Downloaded on 10/16/2025 5:20:47 PM.
This article is licensed under a Creative Commons Attribution-NonCommercial 3.0 Unported Licence.

26 M. Yabushita, N. Shibayama, K. Nakajima and A. Fukuoka, *ACS Catal.*, 2019, **9**, 2101–2109.
27 P. P. Upare, A. Chamas, J. H. Lee, J. C. Kim, S. K. Kwak, Y. K. Hwang and D. W. Hwang, *ACS Catal.*, 2019, **10**, 1388–1396.
28 K. Iris, A. Hanif, D. C. Tsang, J. Shang, Z. Su, H. Song, Y. S. Ok and C. S. Poon, *J. Chem. Eng.*, 2020, **383**, 122914.
29 S. An, D. Kwon, J. Cho and J. C. Jung, *Catalysts*, 2020, **10**, 1236.
30 D. Steinbach, A. Klier, A. Kruse, J. Sauer, S. Wild and M. Zanker, *Processes*, 2020, **8**, 644.
31 I. Graça, M. Bacariza and D. Chadwick, *Microporous Mesoporous Mater.*, 2018, **255**, 130–139.
32 I. Graça, D. Iruretagoyena and D. Chadwick, *Appl. Catal., B*, 2017, **206**, 434–443.
33 I. Graça, M. Bacariza, A. Fernandes and D. Chadwick, *Appl. Catal., B*, 2018, **224**, 660–670.
34 M. M. Antunes, A. Fernandes, D. Falcão, M. Pillinger, F. Ribeiro and A. A. Valente, *Catal. Sci. Technol.*, 2020, **10**, 3232–3246.
35 M. M. Antunes, D. Falcão, A. Fernandes, F. Ribeiro, M. Pillinger, J. Rocha and A. A. Valente, *Catal. Today*, 2021, **362**, 162–174.
36 B. Li, L. Li, Q. Zhang, W. Weng and H. Wan, *Catal. Commun.*, 2017, **99**, 20–24.
37 B. Li, H. Jiang, X. Zhao, Z. Pei and Q. Zhang, *ChemistrySelect*, 2020, **5**, 14971–14977.
38 D.-M. Gao, Y.-B. Shen, B. Zhao, Q. Liu, K. Nakanishi, J. Chen, K. Kanamori, H. Wu, Z. He and M. Zeng, *ACS Sustainable Chem. Eng.*, 2019, **7**, 8512–8521.
39 M. Laiq Ur Rehman, Q. Hou, X. Bai, Y. Nie, H. Qian, T. Xia, R. Lai, G. Yu and M. Ju, *ACS Sustainable Chem. Eng.*, 2022, **10**(6), 1986–1993.
40 M. M. Antunes, A. Fernandes, M. F. Ribeiro, Z. Lin and A. A. Valente, *Eur. J. Inorg. Chem.*, 2020, **2020**, 1579–1588.
41 H. Kitajima, Y. Higashino, S. Matsuda, H. Zhong, M. Watanabe, T. M. Aida and R. L. Smith Jr, *Catal. Today*, 2016, **274**, 67–72.
42 A. I. Rabee, S. D. Le and S. Nishimura, *Chem. – Asian J.*, 2020, **15**, 294–300.
43 S. S. Chen, Y. Cao, D. C. Tsang, J.-P. Tessonnier, J. Shang, D. Hou, Z. Shen, S. Zhang, Y. S. Ok and K. C.-W. Wu, *ACS Sustainable Chem. Eng.*, 2020, **8**, 6990–7001.
44 M. Ventura, J. A. Cecilia, E. Rodríguez-Castellón and M. E. Domine, *Green Chem.*, 2020, **22**, 1393–1405.
45 A. A. Marianou, C. M. Michailof, D. K. Ipsakis, S. A. Karakoulia, K. G. Kalogiannis, H. Yiannoulakis, K. S. Triantafyllidis and A. A. Lappas, *ACS Sustainable Chem. Eng.*, 2018, **6**, 16459–16470.
46 F. Shen, J. Fu, X. Zhang and X. Qi, *ACS Sustainable Chem. Eng.*, 2019, **7**, 4466–4472.
47 J. Ohyama, Y. Zhang, J. Ito and A. Satsuma, *ChemCatChem*, 2017, **9**, 2864–2868.
48 C. Liu, J. M. Carraher, J. L. Swedberg, C. R. Herndon, C. N. Fleitman and J.-P. Tessonnier, *ACS Catal.*, 2014, **4**, 4295–4298.
49 J. M. Carraher, C. N. Fleitman and J.-P. Tessonnier, *ACS Catal.*, 2015, **5**, 3162–3173.
50 N. Deshpande, E. H. Cho, A. P. Spanos, L.-C. Lin and N. A. Brunelli, *J. Catal.*, 2019, **372**, 119–127.
51 Q. Yang and T. Runge, *ACS Sustainable Chem. Eng.*, 2016, **4**, 6951–6961.
52 Q. Yang, M. Sherbahn and T. Runge, *ACS Sustainable Chem. Eng.*, 2016, **4**, 3526–3534.
53 S. S. Chen, D. C. Tsang and J.-P. Tessonnier, *Appl. Catal., B*, 2020, **261**, 118126.
54 S. S. Chen, J. M. Carraher, G. Tuci, A. Rossin, C. A. Raman, L. Luconi, D. C. Tsang, G. Giambastiani and J.-P. Tessonnier, *ACS Sustainable Chem. Eng.*, 2019, **7**, 16959–16963.
55 S. S. Chen, I. K. Yu, D.-W. Cho, H. Song, D. C. Tsang, J.-P. Tessonnier, Y. S. Ok and C. S. Poon, *ACS Sustainable Chem. Eng.*, 2018, **6**, 16113–16120.
56 X. Li, X. Zhang, H. Li and J. Long, *ChemistrySelect*, 2019, **4**, 13731–13735.
57 X. Zhang, H. Li, X. Li, Y. Liu, X. Li, J. Guan and J. Long, *ACS Sustainable Chem. Eng.*, 2019, **7**, 13247–13256.
58 N. Zhang, X. G. Meng, Y. Y. Wu, H. J. Song, H. Huang, F. Wang and J. Lv, *ChemCatChem*, 2019, **11**, 2355–2361.
59 N. Deshpande, L. Pattanaik, M. R. Whitaker, C.-T. Yang, L.-C. Lin and N. A. Brunelli, *J. Catal.*, 2017, **353**, 205–210.
60 Q. Yang, W. Lan and T. Runge, *ACS Sustainable Chem. Eng.*, 2016, **4**, 4850–4858.
61 Q. Yang, S. Zhou and T. Runge, *J. Catal.*, 2015, **330**, 474–484.
62 Y. Wang, J. Wang, Y. Zhang, F. Song, Y. Xie, M. Wang, H. Cui and W. Yi, *Catal. Lett.*, 2020, **150**, 493–504.
63 Z. Guo, C. M. Pedersen, P. Wang, M. Ma, Y. Zhao, Y. Qiao and Y. Wang, *J. Agric. Food Chem.*, 2021, **69**, 5105–5112.
64 S. Lima, A. S. Dias, Z. Lin, P. Brandão, P. Ferreira, M. Pillinger, J. Rocha, V. Calvino-Casilda and A. A. Valente, *Appl. Catal., A*, 2008, **339**, 21–27.
65 R. Otomo, M. Fujimoto, M. Nagao and Y. Kamiya, *Mol. Catal.*, 2019, **475**, 110479.
66 P. A. Son, S. Nishimura and K. Ebitani, *React. Kinet., Mech. Catal.*, 2014, **111**, 183–197.
67 Y. Aizawa, M. Watanabe, T. Iida, R. Nishimura and H. Inomata, *Appl. Catal., A*, 2005, **295**, 150–156.
68 R. O. Souza, D. P. Fabiano, C. Feche, F. Rataboul, D. Cardoso and N. Essayem, *Catal. Today*, 2012, **195**, 114–119.
69 S. Mousa, *Phosphorus Res. Bull.*, 2010, **24**, 16–21.
70 D. Ekeberg, S. Morgenlie and Y. Stenstrøm, *Carbohydr. Res.*, 2007, **342**, 1992–1997.
71 C. Kooyman, K. Vellenga and H. De Wilt, *Carbohydr. Res.*, 1977, **54**, 33–44.
72 S. H. Yalkowsky, Y. He and P. Jain, *Handbook of aqueous solubility data*, CRC press, 2016.
73 G. De Wit, A. Kieboom and H. Van Bekkum, *Carbohydr. Res.*, 1979, **74**, 157–175.
74 I. Delidovich, M. S. Gyngazova, N. Sánchez-Bastardo, J. P. Wohland, C. Hoppe and P. Drabo, *Green Chem.*, 2018, **20**, 724–734.
75 S. J. Angyal, *Aust. J. Chem.*, 1972, **25**, 1957–1966.
76 S. J. Angyal, *Carbohydr. Res.*, 1997, **300**, 279–281.
77 D. Di Tommaso and N. H. de Leeuw, *Phys. Chem. Chem. Phys.*, 2010, **12**, 894–901.
78 M. Makkee, A. Kieboom and H. Van Bekkum, *Recl. Trav. Chim. Pays-Bas*, 1984, **103**, 361–364.